10.37965/jdmd.2026.1471

A Digital-Twin-Enhanced Adversarial Transfer Learning Framework for Fault Diagnosis of Train Axle Box Bearings

Zelin Shen[a], Biao Wang[b,*], Zhuochen Wang[a], Yong Qin[b], Xiaojian Yi[c]

[a]School of Traffic and Transportation, Beijing Jiaotong University, Beijing 100044, China

[b]State Key Laboratory of Advanced Rail Autonomous Operation, Beijing Jiaotong University, Beijing 100044, China

[c]School of Mechanical and Electrical Engineering, Beijing Institute of Technology, Beijing, 100081, China

Received 03 June 2026; Revised 28 July 2026; Accepted 11 August 2026; Published online 12 August 2026

Abstract—Intelligent fault diagnosis methods have become essential for ensuring the secure and dependable functioning of modern railway systems. In particular, digital twin technology offers a highly promising approach to overcome the challenge of limited fault data availability. However, current digital-twin-based fault diagnosis approaches for axle box bearings still exhibit several limitations. 1) They rely on a single digital twin model, which limits the coverage of fault types and working conditions of axle box bearings, reducing the generalization ability of the diagnostic model. 2) They rely on cross-entropy and domain adversarial training without explicitly constraining the feature space, resulting in insufficient inter-class feature discriminability and poor generalization across domains. To address the above limitations, a digital-twin-enhanced adversarial transfer learning framework is proposed for fault diagnosis in axle box bearings. First, a unified feature extractor captures shared feature representations from multiple digital twin models, while class classifiers and domain discriminators are adversarially trained to obtain domain-invariant features. Then, a contrastive learning strategy is applied

* Corresponding author.
E-mail address: wbiao@bjtu.edu.cn (Biao Wang).

to explicitly structure the representation space, enhancing inter-class separability and intra-class compactness. Finally, hard example sampling prioritizes the most confusing positive and negative pairs near decision boundaries, further improving the discriminability of the learned features. Ablation and comparison experiments are conducted using fault simulation data from train axle box bearings, and experimental results show the effectiveness and advantages in leveraging multiple digital twins and improving diagnostic accuracy.

Keywords—axle box bearings; fault diagnosis; digital twin; contrastive learning; hard example sampling.

1. Introduction

As a primary mode of modern transportation, railway transit has made significant advancements in recent years [1]. The increasing velocity and extended service distances of trains introduce mounting complexities in operation and maintenance management [2][3]. By supporting the train's running gear, axle box bearings critically enable smooth wheel-rail interaction and guarantee stable vehicular performance [4]. Even minor defects in the bearing components pose a severe risk of major incidents, which could result in significant monetary setbacks and fatal injuries [5][6]. To maximize the safety and trustworthiness of rail transportation, it is therefore crucial to establish effective fault diagnostic procedures for these bearings. Driven by rapid progress in computing power, deep learning-driven diagnostic techniques have emerged as crucial instruments for defect identification, owing to their robust end-to-end processing strengths [7][8]. For instance, a novel approach presented by Wang et al. [9] utilizes a transferable deep Q-network to achieve intelligent fault detection in planetary gearboxes, effectively overcoming the limitations of variable operating scenarios and sparse datasets by fusing deep reinforcement and transfer learning techniques. Zhang et al. [10] constructed a cross-domain, multi-modal fusion architecture leveraging both thermal images and vibration signals to facilitate gearbox fault diagnosis across varying conditions, thereby bypassing the limitations inherent to single-modal approaches. Li et al. [11] introduced a multi-view graph neural network architecture intended for rotating machine fault detection, which synthesizes multi-sensor data by extracting and combining features from both the time and frequency domains. Huang et al. [12] developed an autoencoder based on interactive generative feature space oversampling to create a wide array of fault samples, thereby mitigating dataset imbalance issues and boosting the robustness of bearing fault diagnosis.

Conventional deep neural networks inherently rely on extensive datasets of fault examples to accurately establish the complicated mapping functions that link raw input signals to distinct failure modes [13]. However, in practice, the axle box bearing is a complex assembly subjected to coupled dynamic loads and environmental influences, and its intricate structural characteristics can give rise to diverse fault patterns. This diversity of fault types, together with the complex and variable working conditions of high-speed trains, makes it challenging to obtain sufficient fault samples. Digital twin is an effective solution for sample augmentation, enabling the generation of labeled fault samples in a virtual environment [14]. In recent years, numerous research endeavors have integrated digital twin technologies into the realm of intelligent fault detection. For example, Qin et al. [15] used a dynamics-based digital twin model with a frequency-domain CycleGAN to generate realistic fault samples, thereby enabling effective bearing fault diagnosis. Feng et al. [16] formulated a graph transfer learning approach utilizing digital twins to identify faults in key components, ensuring efficient domain adaptation from synthetic datasets to empirical records when real-world samples are restricted. Pan et al. [17] introduced a diagnostic approach for key components that integrates experimental measurements with dynamic modeling, utilizing domain-adversarial learning and source domain expansion to enhance feature adaptability and overcome the shortage of physical vehicle fault data. Ming et al. [18] developed a framework augmented by digital twins that executes feature and data transfer to synchronize digitally generated and empirical signals, thereby accomplishing robust fault detection within skewed datasets. While the aforementioned digital twin-based methods have fully utilized twin data to augment datasets and achieved improved diagnostic results, they still face a critical bottleneck. Typically, there is a wealth of unlabeled measurement data, yet labeled samples are scarce due to the labor-intensive nature of tearing down and maintaining key components, coupled with the high financial and temporal costs associated with physical fault testing. Consequently, there remains a lack of approaches capable of effectively leveraging existing limited data through digital twin models to perform reliable fault diagnosis. To solve these problems, the Domain-Adversarial Neural Network (DANN) provides a feasible solution, as it enables the extraction of discriminative fault features from unlabeled data via domain-invariant learning. However, existing studies based on this paradigm still suffer from several limitations.

1) Existing methods typically rely on a single digital twin model as the source domain, which limits the coverage of fault types and working conditions of axle box bearings. The learned diagnostic model often struggles to generalize to bearings under different working conditions. In practice, leveraging multiple digital twin models corresponding to various working scenarios enables the extraction of complementary fault information across domains. Therefore, a comprehensive domain adaptation strategy that explicitly accounts for inter-domain relationships among multiple digital twin models is required to guide intelligent diagnostic networks, thereby improving fault diagnosis performance under varying working condition scenarios.

2) Existing methods typically rely on cross-entropy loss and domain adversarial training to learn feature representations from digital-twin data and measured data, but the structure of the feature space is not explicitly constrained. As a result, class-related features remain insufficiently discriminative, with features of different fault types often overlapping and those of the same fault type dispersing due to domain discrepancies. This weakens the class separability in the source domain and directly hinders the model's generalization to the target domain, ultimately reducing diagnostic accuracy. Therefore, an effective learning mechanism is needed to enhance the inter-class discriminability of features through contrastive learning, ensuring more compact intra-class representations and better-separated inter-class boundaries.

To address these existing constraints, a novel transfer learning framework is developed for intelligent fault diagnosis of train axle box bearings, which leverages multi-digital twin models and domain adaptation. In the digital-twin-enhanced framework, features are extracted via a unified feature extractor, and the class classifier and domain discriminator are pitted against each other to extract domain-invariant features. Next, a distinct contrastive learning mechanism is introduced to precisely regulate the feature representation space, effectively clarifying cross-domain classification boundaries by clustering intra-class data and maximizing inter-class separation. Within this contrastive process, hard example sampling is introduced to prioritize the most confusing positive and negative pairs near the boundary, forcing the model to resolve subtle distinctions and further strengthening the robustness of contrastive alignment. Using axle box bearings of subway trains as a case study for fault diagnosis, the proposed framework demonstrates strong capability in accurately learning and identifying faults under varying working conditions, even when the available condition types are limited. Moreover, comparative results indicate that the proposed framework surpasses existing state-of-the-art methods under such conditions. The main contributions of this work are summarized as follows.

1) A digital-twin-enhanced multi-source domain adversarial network is proposed to align feature representations across multiple digital twin domains and measured data. On one hand, multiple digital twins are treated as complementary source domains, providing richer and more diverse fault information that bridges gaps in the distribution of measured samples. On the other hand, the framework incorporates a gradient reversal layer that forges an adversarial link between the label classifier and domain discriminator, prompting the feature extractor to learn domain-invariant fault features under the guidance of multiple digital twins. Consequently, the diagnostic network is better equipped to generalize, achieving enhanced performance in fault diagnosis under unseen working conditions.

2) A novel contrastive learning strategy is designed to explicitly regularize the feature space by enhancing class-level compactness and separability, which improves feature discriminability and transferability across multiple digital twin source domains. Positive and negative sample pairs are formed by selecting instances of the same and different classes, respectively, within each source domain and among the partially labeled target samples. These pairs are used to compute a contrastive loss, which pulls together representations of the same class and pushes apart representations of different classes. Therefore, this mechanism enhances feature separability, sharpens decision boundaries, and improves cross-domain generalization by jointly leveraging multi-source digital twin labels and partial target supervision.

3) A targeted hard example sampling method is introduced to selectively emphasize highly confusing positive and negative pairs across multiple digital twin source domains during contrastive learning. By focusing on these informative examples from different digital twin sources and the measured target data, the network is encouraged to resolve fine-grained distinctions between similar fault patterns, capturing subtle differences in their feature distributions. Thus, the framework strengthens the robustness and effectiveness of the learned feature representations for fault diagnosis across diverse working conditions and domains, fully exploiting the complementary information provided by multiple digital twin sources.

The rest of this article is formulated as follows. Section 2 introduces the preliminary work, including problem description and transfer learning. Section 3 presents the proposed framework along with the main techniques employed. Section 4 shows the experimental results. Finally, Section 5 concludes this article.

2. Preliminaries

2.1. Problem description

This paper addresses weakly supervised multi-source domain adaptation. The source domains consist of labeled measured data from selected working conditions and labeled digital twin data, whereas measured data from the remaining working conditions constitute the target domain. Only a small subset of the target-domain training data is weakly labeled, while the remaining target samples are unlabeled.

The labeled source datasets are defined as

$$\mathrm{D}_s^m = \{(x_{s_i}^m, y_{s_i}^m)\}_{i=1}^{n_s^m}, \quad m = 1, 2, \ldots, M \tag{1}$$

where the m-th source domain contains n_s^m labeled samples generated by the digital twin model of the m-th component.

The partially labeled dataset is given by

$$\mathrm{D}_t^l = \{(x_{t_k}, y_{t_k})\}_{k=1}^{n_t^l}, \quad n_t^l < n_t \tag{2}$$

where n_t denotes the number of measured samples. In the weakly supervised setting, only a small subset of target samples is labeled, i.e., $n_t^l < n_t$. Due to factors such as structural variations, parameter configurations, working conditions, and modeling assumptions, the datasets collected from different digital twins exhibit distinct distributional characteristics. The label space of each dataset is defined as

$$y = \{1, 2, \ldots, L\} \tag{3}$$

which represents the total number of health states in the dataset.

2.2. Theoretical Foundations of Transfer Learning

Let H denote the hypothesis space, i.e., the set of all classifiers under consideration, and $h \in H$ a particular hypothesis mapping inputs x to predicted labels y. The objective is to analyze the target-domain error $\epsilon_T(h)$ for any $h \in H$ and derive an upper bound based on the labeled source datasets and the partially labeled target dataset.

Define the weighted mixture of source distributions as

$$D_\alpha = \sum_{i=1}^{M} \alpha_i D_S^i, \quad \sum_{i=1}^{M} \alpha_i = 1, \quad \alpha_i \geq 0 \tag{4}$$

where D_S^M is the distribution of the m-th source domain. Then, the expected target-domain error $\epsilon_T(h)$ can be bounded by:

$$\epsilon_T(h) \leq \sum_{m=1}^{M} \alpha_m \epsilon_{S_m}(h) + \frac{1}{2} \sum_{m=1}^{M} \alpha_m d_{H\Delta H}(D_{S_m}, D_T) + \lambda_\alpha \tag{5}$$

Here, λ_α stands for the ideal joint error shared by the target domain and the weighted source mixture. Furthermore, $\epsilon_{S_m}(h)$ indicates the actual classification error of h within the m-th source, while the distribution discrepancy between the *m*-th source and the target is quantified by the $H\Delta H$-divergence, denoted as $d_{H\Delta H}(D_{S_m}, D_T)$.

This mathematical bound illustrates that the error within the target domain is governed by two optimizable factors: the misclassification rates across the source domains and the distributional discrepancy between the source and target data. Simultaneously minimizing both in the feature space is therefore essential to improving generalization on the target domain. In practice, each source domain contains n_s^m labeled samples, and the target domain provides n_t measured samples, among which only n_t^l are labeled. Let $\hat{\epsilon}_{S_m}(h)$ denote the empirical error on the m-th source, and $\hat{D}_{S_m}, \hat{D}_T$ the corresponding empirical distributions. Then, with probability at least $1-\delta$, the finite-sample bound can be expressed as:

$$\epsilon_T(h) \le \left[\sum_{m=1}^{M}\alpha_m \hat{\epsilon}_{S_m}(h)\right]_1 + \left[\frac{1}{2}\sum_{m=1}^{M}\alpha_m d_{H\Delta H}(\hat{D}_{S_m}, \hat{D}_T)\right]_2 + \left[\lambda_\alpha\right]_3 + \left[O\left(\sqrt{\frac{\ln(1/\delta)+v\ln(\sum_{m=1}^{M} n_s^m / v)}{\sum_{m=1}^{M} n_s^m}}\right)\right]_4 \quad (6)$$

Here, v denotes the Vapnik-Chervonenkis (VC) dimension of the hypothesis class H, while the final component accounts for the statistical bias introduced by limited sample sizes. Within this upper bound, the first term aggregates the classification risks across all source domains, whereas the second measures the distribution discrepancy between individual sources and the target; notably, both of these factors can be minimized during training. Conversely, the third term signifies the ideal combined error shared by the target and the mixed source distributions, remaining constant as long as the hypothesis space H is unchanged. Similarly, term (4) captures the effect of limited sample sizes across all domains, which depends solely on data availability and cannot be reduced for a fixed dataset. To address these terms in the present study, a task classifier is trained to correctly predict labeled data from the source domains, thereby minimizing term (1). Domain alignment is further enhanced to reduce term (2) through adversarial learning combined with contrastive learning, promoting feature-level invariance between source and target domains. For term (3), the approach employs a sufficiently large hypothesis space, realized through an adequately sized neural network and an architecture specifically designed for processing vibration signals.

3. Proposed transfer learning network based on multi-digital twin models

The framework of the proposed Digital-Twin-Enhanced Domain Adaptation Network (DT-DAN) is shown in Fig. 1. At the core, a unified feature extraction subnetwork is designed to capture discriminative

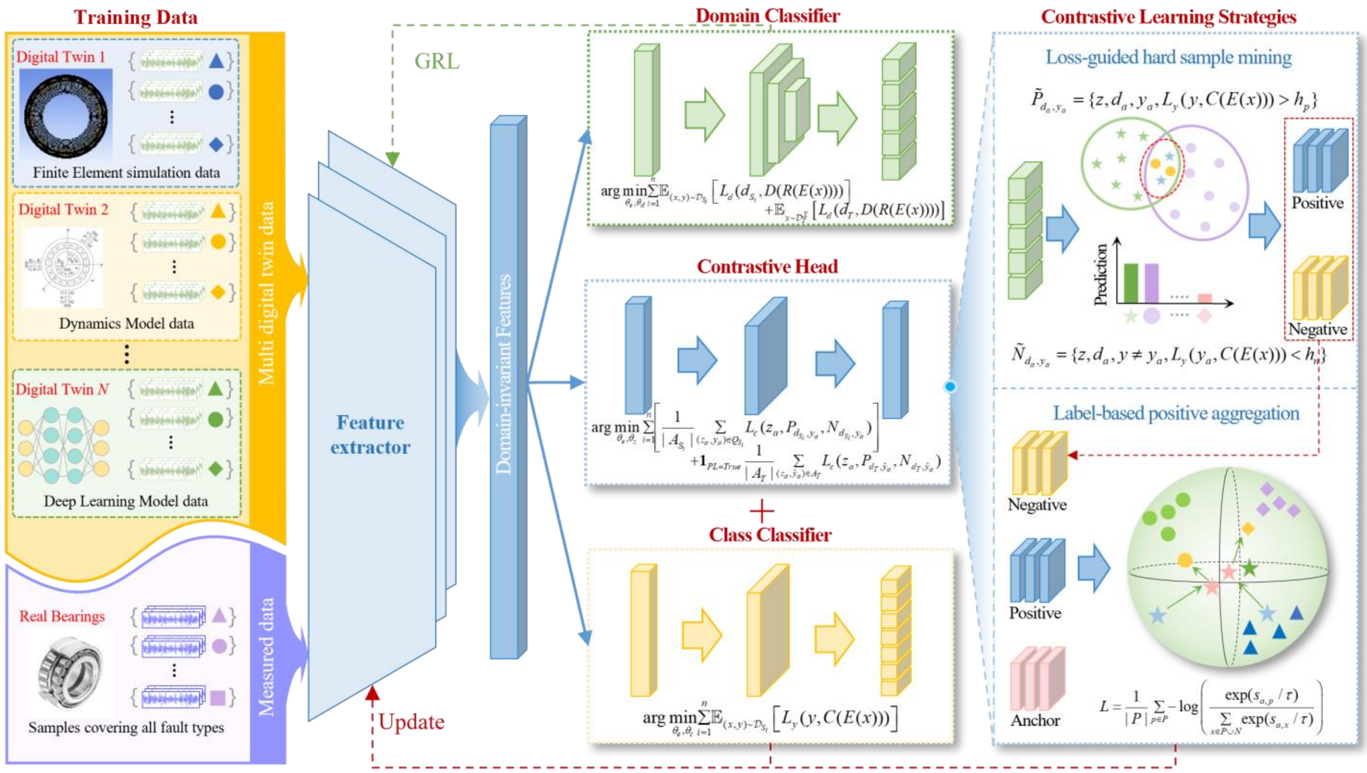

Fig. 1. Digital-Twin-Enhanced Transfer Learning Framework.

representations from multiple digital twin data, which provide complementary fault information across different working conditions. On top of this shared representation space, a class classifier and a domain discriminator are employed to implement adversarial training for extracting domain-invariant features across both digital twin data and measured data. To make full use of the existing supervised information, contrastive learning is introduced to gather intra-class features and separate inter-class features explicitly. In this contrastive learning process, a hard example sampling strategy is adopted to improve the feature distinguishability between different classes further. By jointly reducing classification error, diminishing source–target distribution gaps, and suppressing domain-specific variations, DT-DAN strengthens representation robustness and enhances cross-domain generalization.

3.1. Adversarial Network for Aligning Digital Twin and Measured Data

The foundational architecture of this methodology builds upon Domain-Adversarial Neural Networks (DANN), incorporating a feature extraction module, a label predictor, and a domain discriminator. To reduce the empirical risk across the source data, the encoded representations from the feature extractor $E(\cdot\,|\,\theta_e)$ are routed through a category predictor $C(\cdot|\theta_c)$ equipped with a softmax activation. Subsequently, the weights of both modules are jointly optimized to suppress the categorical cross-entropy loss, which is evaluated between the ground-truth one-hot vectors and the corresponding softmax probability distributions. For multiple source domains, this loss $L_y(y,p)$ is calculated over mini-batches of examples drawn from each source domain distribution $\mathrm{D}_{S_i}, i \in \{1,2,\dots m\}$.

$$\arg\min_{\theta_E,\theta_C} \sum_{i=1}^{n} \frac{1}{N_i} \sum_{j=1}^{N_i} \mathrm{L}_{cls}\left(y_j^{(i)}, C\left(E(x_j^{(i)};\theta_E);\theta_C\right)\right) \tag{7}$$

The feature representations selected by the extractor $E(\cdot|\theta_e)$ may differ significantly between the source and target domains. Minimizing source-domain error alone typically yields a classifier that generalizes poorly to the measured target domain. To mitigate this discrepancy, a domain-adversarial mechanism is employed to enforce feature-level domain invariance by aligning the outputs of the feature extractor across domains. Specifically, a domain classifier is trained to correctly predict the domain label of each example, while the feature extractor is simultaneously optimized to generate domain-invariant features that confuse the domain classifier, effectively aligning source and target feature distributions. This adversarial interaction encourages the network to learn representations that are discriminative for the task while being agnostic to domain-specific variations.

The adversarial dynamic within this network is driven by a softmax-based, multi-class domain discriminator $D(\cdot|\theta_d)$, which processes the representations generated by the feature extractor E. To facilitate adversarial optimization, a gradient reversal layer $R(\cdot)$ is interposed between the extractor and the discriminator, functionally multiplying the backpropagated gradients by a predefined negative scalar $-\lambda_d$. In terms of category assignment, target instances receive a domain label of $d_T = 0$, whereas instances originating from the i-th source are designated as $d_{S_i} = i$ for $i \in \{1,2,\dots,n\}$. Consequently, the variables θ_e and θ_d are trained to optimize the following target function:

$$\min_{\Theta_E,\Theta_D}\left(\sum_{k=1}^{K}\frac{1}{N_k}\sum_{j=1}^{N_k}\mathrm{L}_{dom}\left(d_{S_k},D(R(E(x_j^{(k)})))\right)+\frac{1}{N_T}\sum_{u=1}^{N_T}\mathrm{L}_{dom}\left(d_T,D(R(E))\right)\right) \tag{8}$$

To achieve this optimization, the network utilizes a categorical cross-entropy function L_d, which structurally mirrors the primary classification loss L_y but operates on domain identifiers rather than specific task categories. Defining d as the actual one-hot encoded domain vector and p as the predicted probability distribution yielded by the domain discriminator's softmax layer, this loss is formulated as follows

$$L_d(d,p)=-\sum_{i=1}^{n}d_i\log p_i \tag{9}$$

3.2. Leveraging label information more efficiently via contrastive learning

The adversarial loss introduced primarily enforces domain invariance but does not explicitly exploit labeled information from the source domains. The DANN that jointly optimizes the adversarial loss and the task loss makes the features discriminative within each source domain but does not guarantee that same-class samples from different source domains are mapped close to one another. To better leverage source labels, a supervised contrastive loss is introduced to encourage representations of examples sharing the same class label to be pulled closer in the embedding space, while pushing apart those with different labels. The principle of this supervised contrastive learning process is illustrated in Fig. 2. This loss thereby utilizes both positive and negative cross-source label information, complementing the adversarial alignment. Formally, this process operates on pairs of projected representations z derived from inputs, where each anchor $a \in A$ is paired with a positive $p \in P$ having the same label and a negative $n \in N$ with a different label. DT-DAN extends this formulation by allowing additional constraints on pair selection, such as restricting examples to come from the same domain, different domains, or any domain, and whether to incorporate pseudo-labeled target instances. One anchor–positive pair (a,p) and one anchor–negative pair (a,n) can be formed for both within-source and cross-source cases, with multiple pairs being constructed analogously.

The objective for supervised contrastive learning utilizes a multi-positive variant of the InfoNCE framework. For a specific anchor embedding z, accompanied by its corresponding positive subset $\mathcal{P}$ and negative subset $\mathcal{N}$, a temperature scaling factor τ, and the cosine similarity metric denoted as

$$\mathrm{sim}(z_1, z_2) = \frac{z_1^{\cdot} z_2}{\| z_1 \| \| z_2 \|} \tag{10}$$

The loss is expressed as

$$L_c(z, \mathcal{P}, \mathcal{N}) = \frac{1}{|\mathcal{P}|} \sum_{z_p \in P} \left[\log\left(\sum_{z_k \in \mathcal{N} \cup \{z_{\mathcal{P}}\}} \exp\left(\frac{\mathrm{sim}(z, z_k)}{\tau} \right) \right) - \frac{\mathrm{sim}(z, z_{\mathcal{P}})}{\tau} \right] \tag{11}$$

For each anchor, the numerator encourages similarity with its positives, while the denominator simultaneously contrasts against positives and negatives. This formulation is mathematically equivalent to a log-softmax classifier distinguishing positives from negatives, with the averaging over multiple positives placed outside the logarithm for improved performance. The overall objective then aggregates over all anchors from source domains and, in some instantiations, pseudo-labeled target anchors:

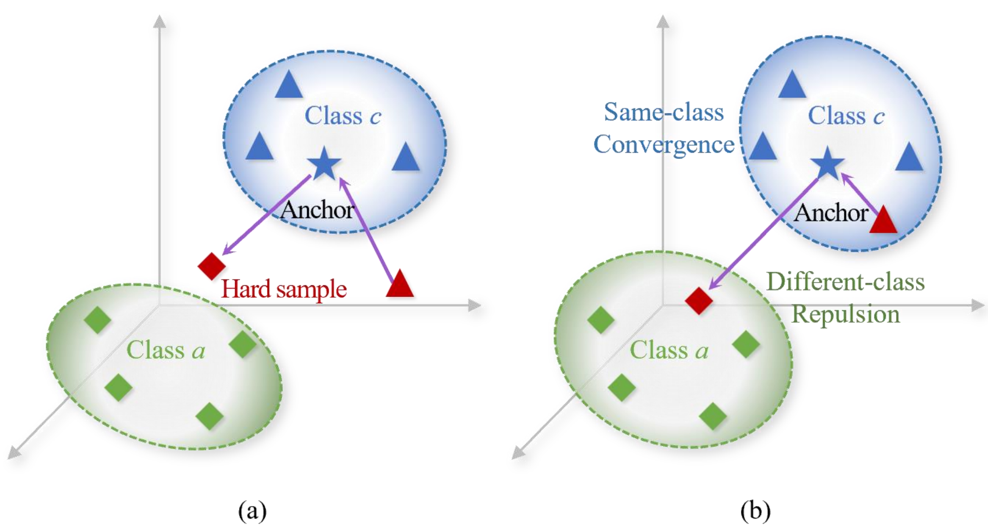

Fig. 2. Schematic Diagram of Contrastive Learning. (a) Before Implementing Contrastive Learning. (b) After Implementing Contrastive Learning.

$$\arg\min_{\theta_e, \theta_z} \sum_{i=1}^{n} \left[\frac{1}{|A_{S_i}|} \sum_{(z_a, y_a) \in A_{S_i}} L_c(z_a, \mathcal{P}_{d_{S_i}, y_a}, \mathcal{N}_{d_{S_i}, y_a}) \right] + \mathbf{1}_{PL=True} \frac{1}{|A_T|} \sum_{(z_a, \hat{y}_a) \in A_T} L_c(z_a, \mathcal{P}_{d_T, \hat{y}_a}, \mathcal{N}_{d_T, \hat{y}_a}) \tag{12}$$

To formalize pair construction under different DT-DAN instantiations, an auxiliary set $\mathcal{V}$ is defined, containing each example's input x, its class label y (or pseudo-label $\hat{y}$ for target instances), and its domain label d. Given labeled source samples $S_i \sim D_{S_i}$ for $i \in \{1,\ldots,n\}$, unlabeled target samples $T_{\text{train}} \sim D_T$, and projected representations $z = Z(E(x);\theta_z)$, the following sets are defined:

$$\mathrm{V}_{src} = \{(x,y,d) | (x,y) \in S_i, i \in \{1,2,\ldots,n\}, d = d_{S_i}\} \tag{13}$$

$$\mathrm{V}_{tgt} = \{(x,\tilde{y},d) | \; x \in T_{train}, \tilde{y} = \arg\max C(E(x)), d = d_T\} \tag{14}$$

$$\mathrm{V}_{all} = \mathrm{V}_{src} \cup \mathrm{V}_{tgt} \tag{15}$$

Using V, anchor sets for each source domain and the target domain are defined as:

$$A_{S_i} = \left\{ \left(Z(E(x)), y \right) | (x, y, d_{S_i}) \in \mathrm{V} \right\} \tag{16}$$

$$A_T = \left\{ \left(Z(E(x)), \hat{y} \right) | (x, \hat{y}, d_T) \in \mathrm{V} \right\} \tag{17}$$

Positive and negative sets are instantiated according to the specific framework configuration, including within-source, cross-source, or any-source sampling. For instance, in the cross-source label-contrastive learning configuration, contrastive pairs are constructed across different source domains to exploit inter-domain supervision. Positives are selected from other domains that share the same label as the anchor, while negatives are sampled from different domains with different labels. This setup explicitly encourages alignment of class-consistent representations across domains while maintaining inter-class separability. In the context of multi-digital twin models, the label spaces of the digital twin domains and real measurement domains are complementary rather than completely disjoint. Therefore, cross-source label-contrastive learning can be effectively applied by forming positive pairs between the digital twin data and the real measurement data with the same label, while negatives are drawn from samples of different labels across any domain.

$$\mathrm{P}_{d_a, y_a} = \left\{ Z(E(x)) | (x, y_a, d) \in \mathrm{V}, d \neq d_a \right\} \tag{18}$$

$$\mathrm{N}_{d_a, y_a} = \left\{ Z(E(x)) | (x, y, d) \in \mathrm{V}, d \neq d_a, y \neq y_a \right\} \tag{19}$$

Furthermore, weakly supervised labels from the measured target data can also be incorporated by including target instances $(x, \tilde{y}, d_T)$ with weak label $\tilde{y}$ into the auxiliary set V. To account for label uncertainty, each weakly labeled instance is assigned a confidence weight $w_p \in [0,1]$, and the supervised contrastive loss for an anchor a becomes

$$L_c(a) = -\frac{1}{|P_a|} \sum_{p \in \mathrm{P}_a} w_p \cdot \log \frac{\exp(\mathrm{sim}(z_a, z_p)/\tau)}{\sum_{b \in \mathrm{P}_a \cup \mathrm{N}_a} \exp(\mathrm{sim}(z_a, z_b)/\tau)} \tag{20}$$

By weighting weakly supervised samples in this way, the framework benefits from partial target-domain supervision while maintaining robust intra-domain contrastive alignment.

3.3. Hard example sampling for contrastive learning

To improve the effectiveness of contrastive learning, a hard example sampling strategy is introduced. In contrastive learning, not all positive and negative pairs contribute equally to feature learning; examples near the decision boundary are more informative for distinguishing classes. Therefore, focusing on these “hard” examples can accelerate training and enhance feature discriminability. The effect of the pair construction is illustrated in Fig. 3. For each anchor of domain d_a and label y_a hard positives are defined as examples from the same domain with the same label but currently associated with a high task classification loss, indicating they are close to being misclassified. Hard negatives are examples from the same domain with a different label but predicted with a low task loss for the anchor’s class, indicating they are likely to be confused with the anchor. Formally, the hard positive and negative sets P_{hard} and N_{hard} are defined as:

10.37965/jdmd.2026.1471

$$\mathrm{P}_{hard}^{(d_a,y_a)} = \left\{ Z(E(x)) \middle| (x, y_a, d) \in \mathrm{V}, d \neq d_a, \hat{y} \neq y_a \right\} \tag{21}$$

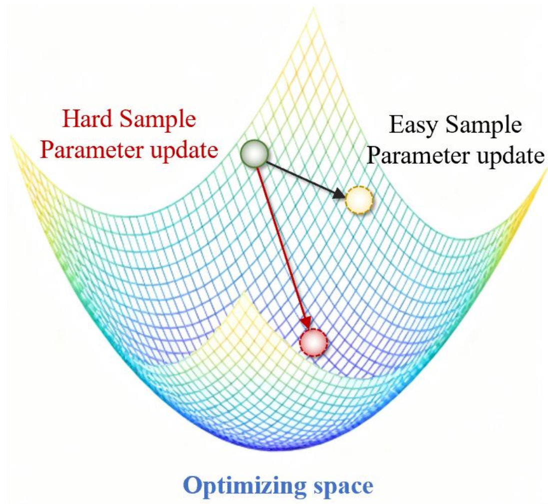

Fig. 3. Schematic Diagram of Hard example sampling.

$$\mathrm{N}_{hard}^{(d_a,y_a)} = \left\{ Z(E(x)) \middle| (x, y, d) \in \mathrm{V}, d \neq d_a, y \neq y_a, \hat{y} = y_a \right\} \tag{22}$$

However, in practice, it is not guaranteed that truly misclassified positive and negative examples will always exist, as the task classifier may eventually make correct predictions during later training stages. To address this, a relaxed hard example selection strategy is proposed. Specifically, based on the softmax cross-entropy loss, the top-k_1 hardest positives and top-k_2 hardest negatives are selected. For an anchor with domain d_a and label y_a, hard positives are defined as samples from the same domain with the same label that currently have a high task classification loss, indicating that they lie near or beyond the decision boundary and are close to being misclassified. Conversely, hard negatives are defined as samples from the same domain but with a different true label, whose predicted loss with respect to the anchor's label y_a is small, indicating that they are likely to be confused with the anchor and to lie near the decision boundary on the wrong side.

$$\mathrm{P}_{hard}^{(a)} = \left\{ Z(E(x)) \mid (x, y_a, d_a) \in \mathrm{V}, \mathrm{L}_{cls}\left(y_a, C(E(x))\right) > h_p \right\} \tag{23}$$

$$\mathrm{N}_{hard}^{(a)} = \left\{ Z(E(x)) \middle| (x, y, d_a) \in \mathrm{V}, y \neq y_a, \mathrm{L}_{cls}\left(y_a, C(E(x))\right) < h_n \right\} \tag{24}$$

where h_p and h_n are thresholds selected to obtain a predefined number of hard positives and negatives.

By concentrating on these challenging examples, the contrastive learning loss can more effectively pull together representations of the same class and push apart representations of different classes within each domain, improving intra-domain feature alignment and overall transfer performance.

4. Experimental verification

In this section, train axle box bearing fault simulation experiments are conducted under various working conditions to verify the effectiveness of the proposed transfer learning framework. Furthermore, the proposed framework is also compared with several state-of-the-art methods.

4.1 Experiment introduction

To verify the proposed digital-twin-enhanced transfer learning framework for train axle box bearing fault diagnosis across different working conditions, three complementary digital twins and measured data are employed for model training and evaluation. The three digital twins are developed from different modeling perspectives to provide a comprehensive representation of bearing behavior: (DT1) a finite element (FE) model, (DT2) a dynamics-based mechanistic model (DMM), and (DT3) a deep-learning-based generative model (DGM).

To clarify the domain assignment and the relationship among the datasets, the measured data are divided according to their working conditions. Measured data collected under a subset of known working conditions

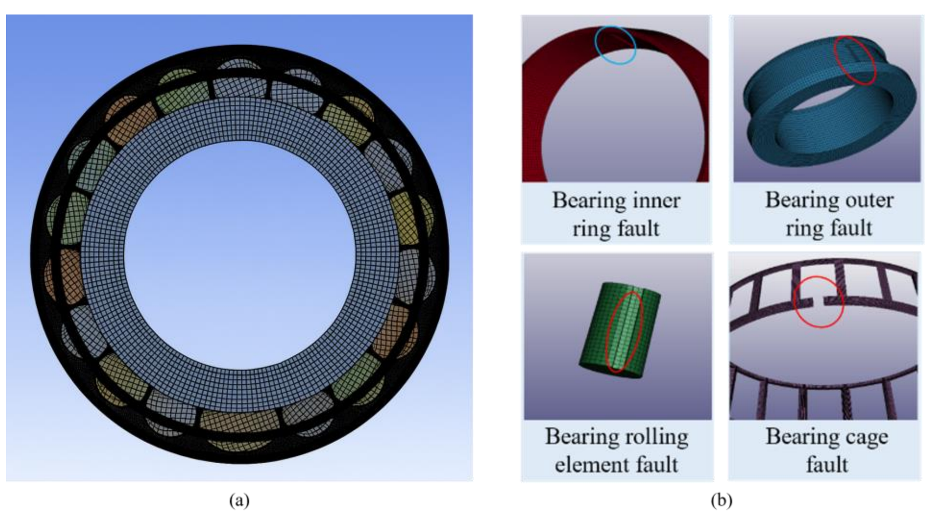

Fig. 4. Axle box bearing model and its fault simulations. (a) model after meshing. (b) summary of fault types.

are selected as the measured source domain. These source-condition measured data are used to calibrate and validate the physics-based digital twins, including DT1 and DT2, and to train the data-driven generative digital twin, DT3. The three digital twins then generate additional labeled fault samples from complementary modeling perspectives, and the resulting datasets are treated as three digital-twin source domains. Therefore, the collection of source domains consists of both labeled measured data under the selected source conditions and labeled samples generated by DT1, DT2, and DT3.

Measured data collected under the remaining working conditions are assigned to the target domain and are not used to construct, calibrate, or train the digital twin models. The target-domain data are further divided into a training set and an independent test set. The target-domain training set contains a small number of weakly labeled samples and a larger number of unlabeled samples, both of which participate in model training, while the independent test set is used solely for final performance evaluation. Under this setting, the proposed framework transfers diagnostic knowledge learned from the measured and digital-twin source domains to

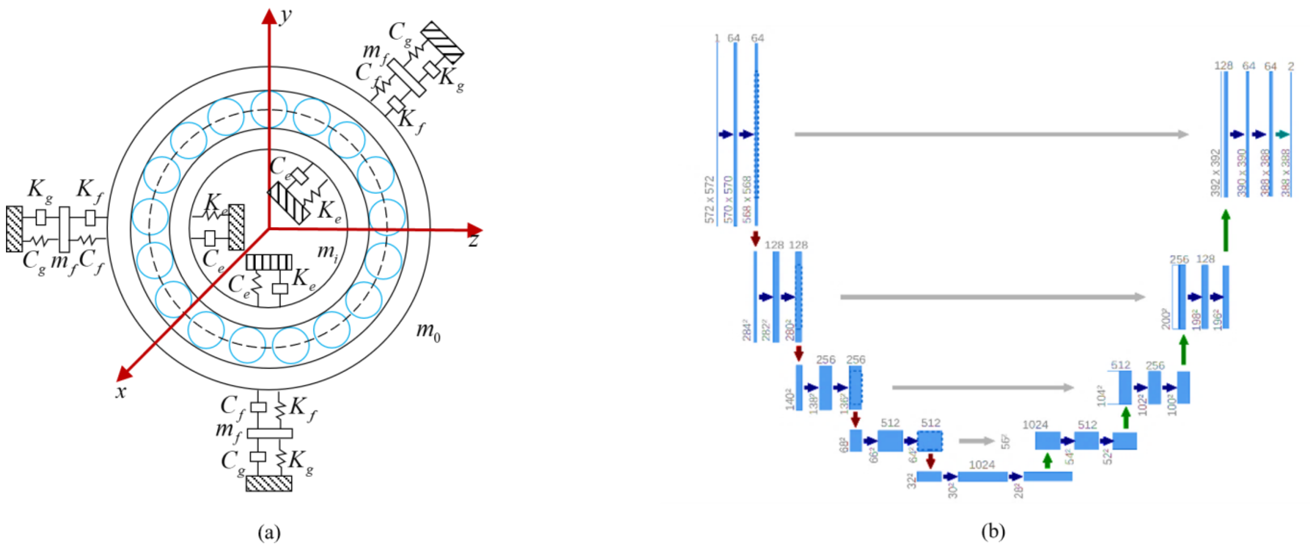

Fig. 5. Sample Generation Method. (a) Dynamics-based Mechanistic Model [19]. (b) Deep learning-based Model [20]

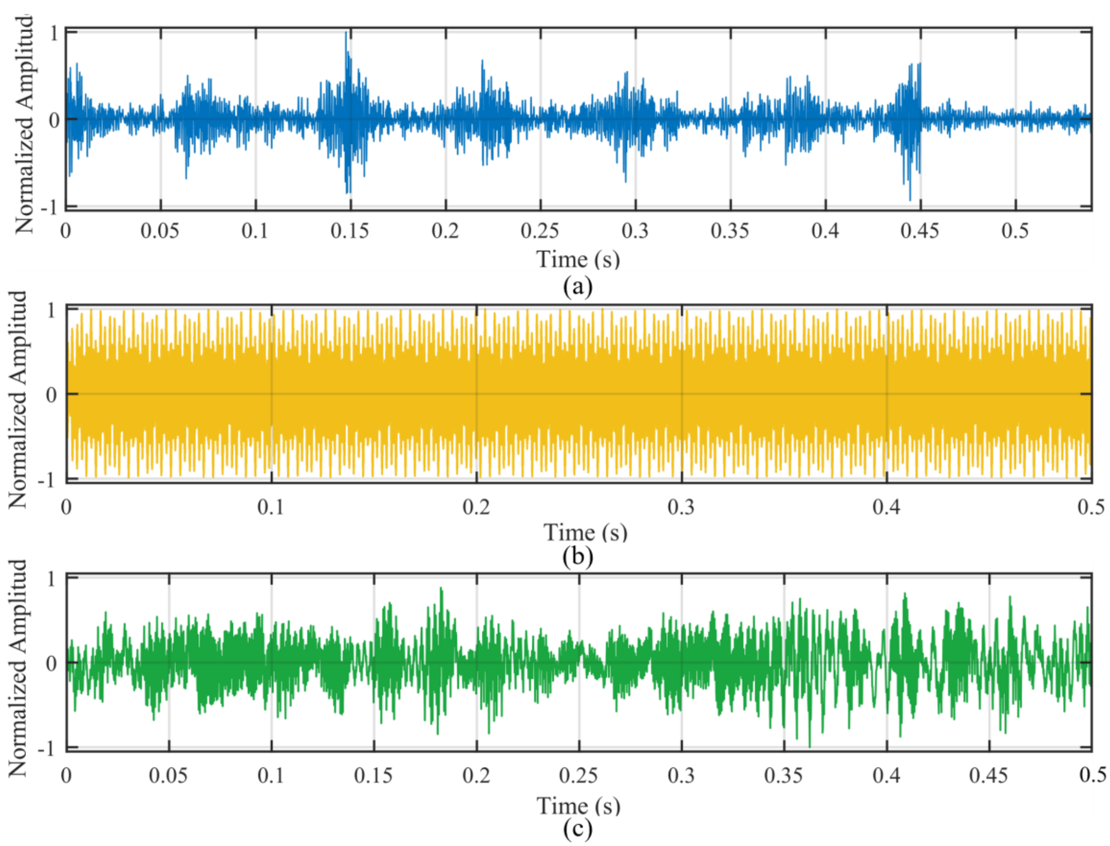

Fig. 6. Time-domain signals generated by the twin models: (a) DT1; (b) DT2; and (c) DT3.

target working conditions that are not included in source-domain training. The detailed configurations of the three digital twin models are introduced below.

1) DT1: As illustrated in Fig. 4, FE analysis is conducted on a single-row SKF32213 bearing. The bearing's dimensional parameters are obtained from official SKF documentation. To ensure

computational efficiency without compromising accuracy, geometric features with negligible influence such as chamfers, lubrication holes, and the complex cage structure are omitted during modeling. The bearing material is defined with standard steel properties, including Young's modulus, Poisson's ratio, and density. The model is discretized using 8-node hexahedral elements (SOLID164), and locally refined meshes are applied at the contact interfaces between rolling elements and raceways to capture stress concentrations. Rigid–flexible contact pairs are defined to permit free rolling motion under a specified friction coefficient. Five health states are simulated: normal, outer ring fault, rolling element fault, inner ring fault, and cage fault.

2) DT2: As shown in Fig. 5(a), the DMM is a multi-body coupled dynamic model that comprehensively accounts for the multi-directional contact stiffness and damping between rollers and raceways. It captures nonlinear contact dynamics and boundary interactions under varying operating conditions, generating response data that bridge the gap between FE simulations and physical experiments.

3) DT3: Depicted in Fig. 5(b), the DGM adopts a conditional diffusion-based generative framework that incorporates prior information such as working conditions and fault types to synthesize diverse and realistic fault samples. This model enhances the variability of fault patterns and improves the generalization capability of the diagnostic framework. These three digital twins collectively provide comprehensive coverage of fault types and working conditions, enabling the learning of robust and domain-invariant representations within the proposed transfer learning framework.

Fig. 6 compares representative normalized time-domain signals generated by the three digital twin models. As shown in Fig. 6(a), the FE-based digital twin produces intermittent impact-dominated responses characterized by localized high-amplitude bursts and oscillatory wave packets. These characteristics reflect the transient structural responses caused by local defect contact, stress redistribution, and vibration propagation within the bearing structure. In contrast, the dynamics-based mechanistic digital twin in Fig. 6(b)

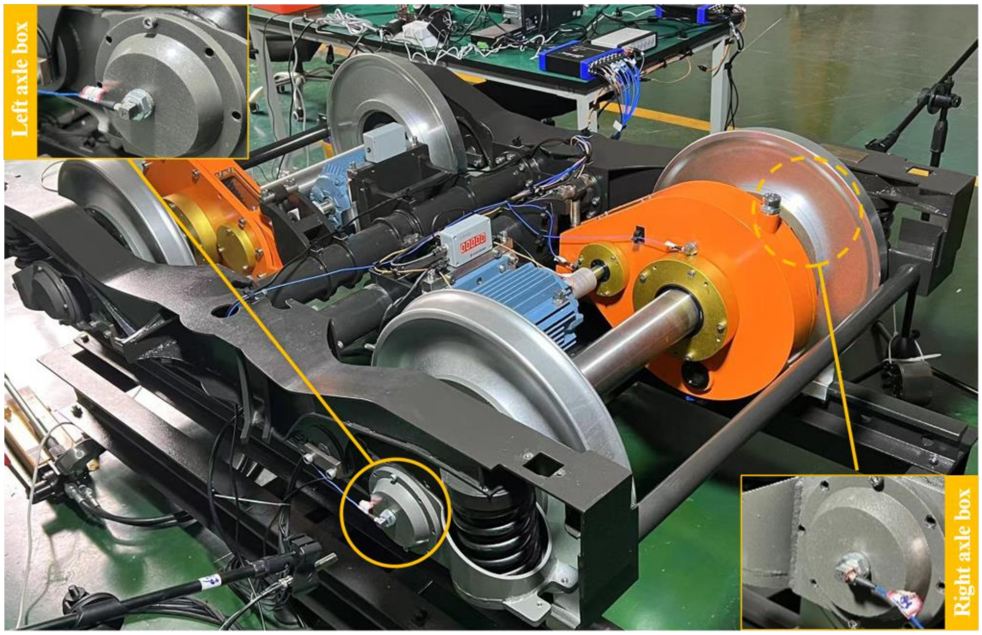

Fig. 7. Measured data collection platform.

Fig. 8. Faults of axle box bearings.

generates densely repeated and strongly periodic oscillations with a relatively stable envelope. Such signals primarily represent the deterministic kinematic excitation, periodic roller–raceway interactions, and nonlinear stiffness–damping coupling of the bearing system. The diffusion-based generative digital twin shown in Fig. 6(c) produces more irregular and nonstationary waveforms, with pronounced variations in amplitude, envelope, and local temporal morphology, thereby increasing the stochastic diversity of the generated fault samples.

The three types of digital twin data therefore provide complementary source-domain information. The FE-based digital twin emphasizes physically interpretable local structural responses and transient impact characteristics, while the dynamics-based digital twin describes periodic fault excitation and system-level nonlinear dynamic behavior. The diffusion-based digital twin further enriches the source domain by introducing variations in signal morphology and sample distribution that cannot be fully represented by deterministic physical models. Combining these datasets broadens the coverage of fault patterns and working-condition variations in the source-domain feature space. This complementary information prevents the diagnostic model from overfitting to the specific characteristics of a single digital twin and facilitates the learning of more robust and transferable fault representations, thereby improving generalization to measured data under unseen working conditions.

By integrating DT1, DT2, and DT3, a multi-digital twin dataset is constructed. Together with measured samples under known working conditions, this dataset constitutes the source domain for model training. The measured data are further described as follows. As shown in Fig. 7, they are collected from fault simulation experiments conducted on a 1:2 scaled physical prototype of a real metro bogie, which is equipped with a frequency converter to regulate motor rotational speeds and an electro-hydraulic loading device to apply different lateral loads. The fault types of axle box bearings are illustrated in Fig. 8. During the experiments,

Table 1

Overview of working conditions.

Serial Number	Load/Speed	Serial Number	Load/Speed
A1	0 kN/20 Hz	B3	-10 kN/40 Hz
A2	10 kN/20 Hz	C1	0 kN/60 Hz
A3	-10 kN/20 Hz	C2	10 kN/60 Hz
B1	0 kN/40 Hz	C3	-10 kN/60 Hz
B2	10 kN/40 Hz	-	-

Table 2

Overview of the dataset.

Data Source	Working condition	Number of Fault Types	Number of Samples
DT1	A1, A2, A3 B1, B2, B3 C1, C2, C3	5	1800
DT2	A1, A2, A3 B1, B2, B3 C1, C2, C3	5	1800
DT3	A1, A2, A3 B1, B2, B3 C1, C2, C3	5	1800
Measured Data	A1, A2, A3 B1, B2, B3 C1, C2, C3	5	1800

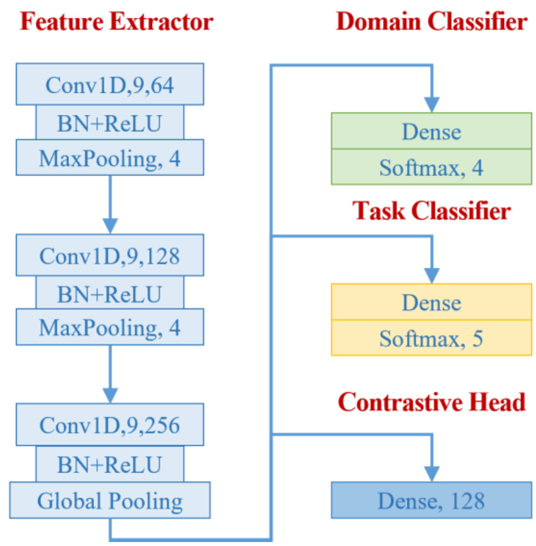

Fig. 9. Network configuration.

three-axis vibration signals of the axle box bearings are recorded at a sampling rate of 64 kHz, and the corresponding working conditions are summarized in Table 1. In Table 1, A, B, and C denote the three rotational-speed conditions, whereas 1, 2, and 3 denote the three load conditions. To provide a comprehensive overview, Table 2 summarizes all datasets used in the experiments, including the data generated by the three digital twin models and the measured samples collected under different working conditions. Based on these datasets, the proposed network is subsequently trained and optimized. All experiments are conducted on a workstation equipped with an Intel Core i7-14700KF CPU and an NVIDIA GeForce RTX 4070 Ti GPU. The diagnostic model is implemented in Python using the PyTorch deep learning framework. The network parameters are optimized using the Adam optimizer for 500 epochs, and the input sequence length of each training sample is set to 3200 sampling points. The weights of the classification loss, domain-adversarial loss, and contrastive loss are set to 1:0.5:0.1. The hyperparameter tuning results obtained through cross-validation are presented in Fig. 9. For the hard example sampling strategy, the sample-wise classification losses are first calculated within each mini-batch. The 90th percentile of these losses is used as an adaptive threshold T_h, and samples satisfying $L_i^{ce} \geq T_h$, corresponding to the top 10% hardest samples, are selected for subsequent contrastive learning. The temperature parameter in the contrastive loss is set to $\tau = 0.1$. These hyperparameters are determined through cross-validation.

4.2 Benefits of Multi-Digital-Twin Augmentation

An ablation study is conducted to evaluate the effectiveness of multi-digital-twin augmentation. In this study, a series of transfer learning networks is constructed, with the number of source domains progressively increased. Specifically, three source-domain configurations are compared: measured source data combined with one digital twin, two digital twins, and three digital twins. For each transfer task, the labeled measured data collected under the selected known working conditions and the labeled samples generated by the digital twins are treated as the source domains. The measured source-domain data and digital-twin data are jointly

Table 3

Diagnostic Results for Varying Numbers of Digital Twins under Rotational Speed Transfer

Task	DT1(FE)	DT2(DMM)	DT3(DGM)	Diagnosis accuracy
A, B→C	√	×	×	92.81%±0.4%
	√	√	×	93.57%±0.5%
	√	√	√	**94.28%±0.3%**
A, C→B	√	×	×	94.19%±0.5%
	√	√	×	95.74%±0.3%
	√	√	√	**96.76%±0.3%**
B, C→A	√	×	×	94.31%±0.3%
	√	√	×	94.76%±0.4%
	√	√	√	**95.41%±0.3%**

Note: In each task, the working conditions on the left side of "→" are used as the source conditions, and the condition on the right side is used as the target condition. The reported accuracy is calculated using the independent target-domain test set.

Table 4

Diagnostic Results for Varying Numbers of Digital Twins under Load Transfer

Task	DT1(FE)	DT2(DMM)	DT3(DGM)	Diagnosis accuracy
1, 2→3	√	×	×	93.34%±0.4%
	√	√	×	94.16%±0.3%
	√	√	√	**95.28%±0.4%**
1, 3→2	√	×	×	93.51%±0.4%
	√	√	×	94.98%±0.2%
	√	√	√	**96.39%±0.3%**
2, 3→1	√	×	×	93.75%±0.3%
	√	√	×	94.64%±0.4%
	√	√	√	**95.77%±0.4%**

Note: The load conditions on the left side of "→" are used as the source conditions, and the load condition on the right side is used as the target condition. The reported accuracy is calculated using the independent target-domain test set.

used for task classification, supervised contrastive learning, and domain-adversarial training. Measured data collected under the held-out working conditions constitute the target domain and are further divided into a target-domain training set and an independent target-domain test set. For each transfer task, 5% of the target-domain training samples are randomly selected without replacement as weakly supervised samples, while the remaining 95% are treated as unlabeled samples. After training, all models are evaluated on the same independent target-domain test set, which consists of measured samples from the held-out working conditions and is used solely for final performance evaluation. To ensure reliability, the network training and testing procedures are repeated ten times in total. Tables 3 and 4 report the average accuracy and standard deviation of the networks in fault diagnosis tasks. As shown by the results, the diagnostic performance of the models gradually improves as the number of twins increases. Under both rotational speed transfer and load transfer scenarios, the inclusion of digital twin-generated data effectively enhances the generalization capability of the diagnostic networks. This is because the digital twins generate supplementary samples that occupy regions of the feature space underrepresented by experimental data alone, thereby narrowing the distribution gap between the source and target domains. Specifically, the FE and dynamic model-based twins capture physically accurate fault dynamics under different working conditions. Meanwhile, the deep learning-generated twins enrich the variability of the signal patterns. In conclusion, the ablation experiments demonstrate that leveraging multiple source domains significantly improves the diagnostic accuracy and robustness of axle box bearings under unseen working conditions.

4.3 Effects of contrastive learning and the hard example sampling strategy

To evaluate the contribution of the proposed contrastive learning module and the hard example sampling strategy, an ablation study is conducted for axle box bearing fault diagnosis. For each transfer task, the labeled measured data collected under the selected known working conditions and the labeled samples generated by the digital twins are treated as the source-domain data. The measured data collected under the held-out working conditions constitute the target domain and are divided into an unlabeled target-domain training set

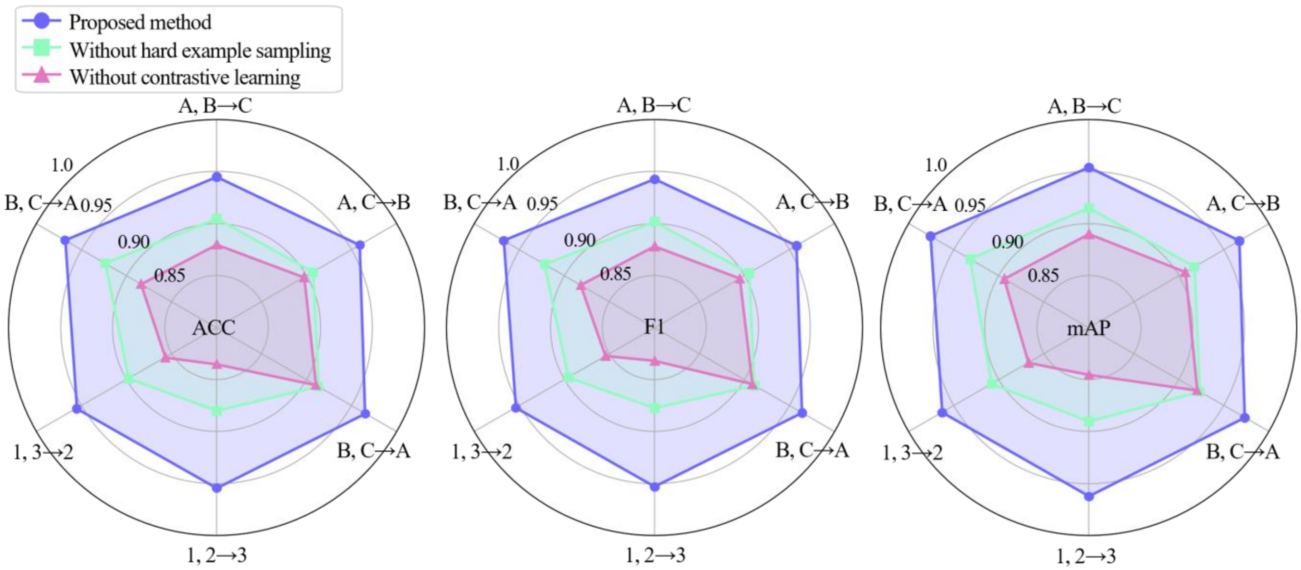

Fig. 10. Diagnostic performance of different sampling methods.

and an independent target-domain test set. Three strategies are compared: conventional training without contrastive regularization, contrastive learning with randomly constructed positive and negative pairs, and contrastive learning combined with the proposed hard example sampling strategy.

During training, the supervised contrastive loss is constructed only from labeled measured and digital-twin source-domain samples, whereas the unlabeled target-domain samples participate only in domain-adversarial alignment. After training, all models are evaluated on the same independent target-domain test set, which does not overlap with the target-domain samples used for domain-adaptation training. Fig. 10 presents the diagnostic results under the three strategies. As shown in Fig. 10, conventional training without contrastive learning achieves the lowest diagnostic accuracy. Although the task classification loss enables the model to distinguish fault classes in the labeled source domains, and domain-adversarial learning reduces the overall distribution discrepancy between the source and target domains, these objectives do not explicitly constrain the class-level structure of the feature space. Consequently, features belonging to the same fault class but originating from different measured and digital-twin source domains may remain dispersed, whereas features from different fault classes may still overlap after domain alignment. Such a feature distribution leads to ambiguous classification boundaries and limits the transferability of the diagnostic model. Introducing contrastive learning significantly improves diagnostic performance. During contrastive learning, labeled source-domain samples with the same fault label are constructed as positive pairs, whereas samples with different fault labels are constructed as negative pairs. Minimizing the contrastive loss pulls positive pairs closer together and pushes negative pairs farther apart in the feature space. In this way, contrastive learning explicitly enhances intra-class compactness, inter-class separability, and the classification margin across the measured and digital-twin source domains. It also suppresses domain-specific variations that are unrelated to fault categories and encourages samples with the same health state to form consistent feature clusters across different source domains.

Building on this, the combination of contrastive learning with hard example sampling achieves the highest accuracy, particularly under unseen working conditions. With random pair construction, a large number of easily distinguished positive and negative pairs contribute only limited information to the optimization process and may dominate the contrastive loss. In contrast, the proposed hard example sampling strategy preferentially selects hard positive pairs that remain relatively far apart and hard negative pairs that are relatively close in the feature space. By jointly leveraging these mechanisms, the network effectively learns transferable representations and mitigates the domain shift between source and target working conditions. Under traditional random sampling, the optimization direction of the loss function is diluted by a large number of simple samples, making it difficult to focus on the core contradiction of class differentiation and leading to a significant decline in diagnostic accuracy. Overall, the ablation results demonstrate that contrastive learning provides the fundamental improvement by explicitly constructing a class-discriminative feature space with enhanced intra-class compactness and inter-class separability, whereas hard example sampling further refines this feature space by emphasizing informative sample pairs near the decision boundaries.

4.4 Comparison with state-of-the-art methods

To verify the superiority of the multi-source domain adversarial transfer learning framework based on the digital twin model, this study conducted fault diagnosis on the axle box bearings, and compared the diagnostic accuracy of the proposed method with four existing methods. Table 5 presents brief descriptions of each method, and Fig. 11 reports diagnostic accuracy across different transfer learning tasks. The experimental results demonstrate that the proposed method consistently outperforms the existing methods in all tasks.

Table 5

Descriptions of the comparative methods

Methods	Descriptions
Method A	Method A is a baseline that only applies a multi-source domain adversarial network without addressing disjoint labels.
Method B	Method B (CDAN) improves class separability by conditioning domain alignment on label predictions.[21]
Method C	Method C (M^3SDA) enhances transfer by aligning higher-order feature moments across domains.[22]
Method D	Method D (MDD) sharpens decision boundaries by minimizing margin disparity discrepancy.[23]

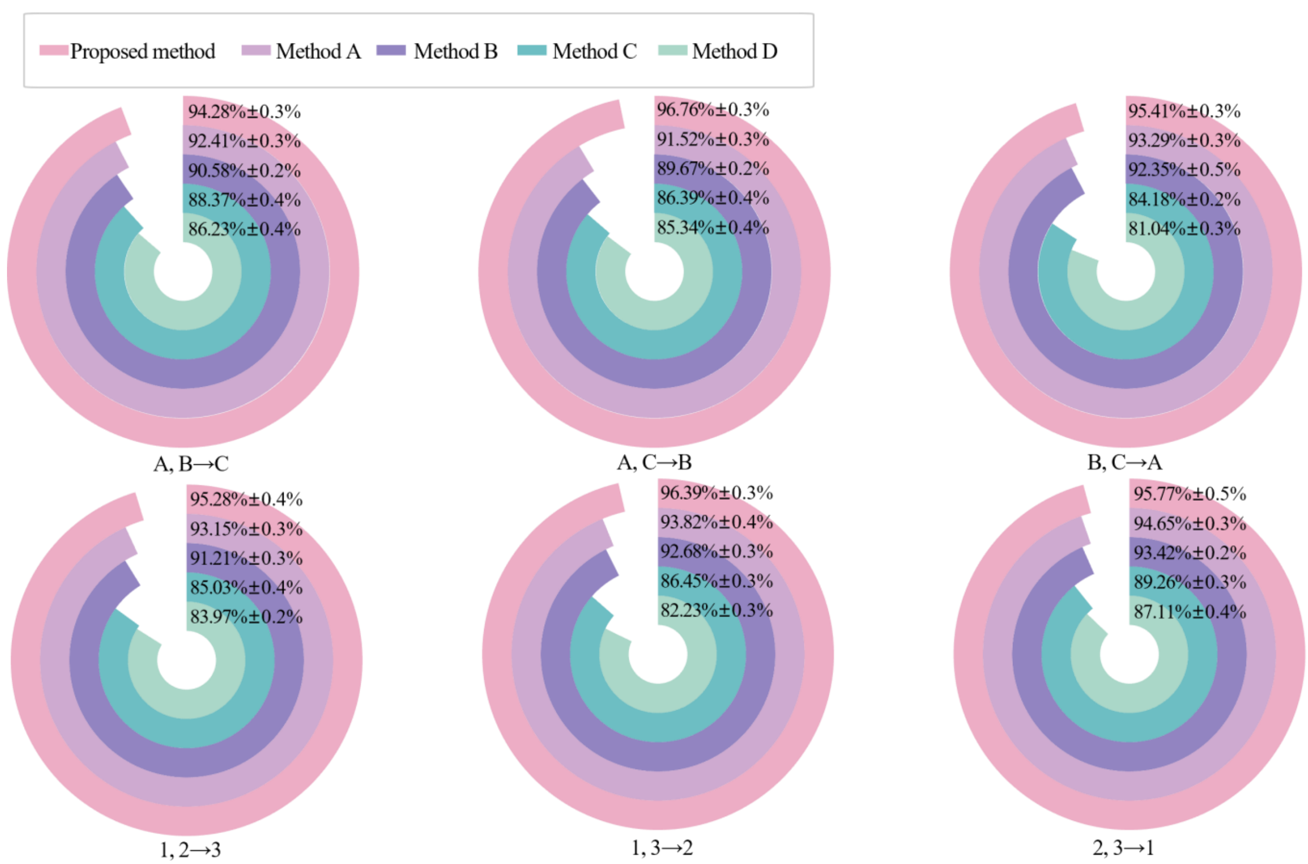

Fig. 11. Comparison results of the proposed method and the other existing methods.

Specifically, Method A, serving as the baseline, employs only a multi-source domain adversarial network and does not address the issue of non-overlapping labels between domains, resulting in the poorest performance in distinguishing complex fault categories. Method B improves class separability by conditioning domain alignment on label predictions; however, it still depends on the quality of the predicted labels and struggles to effectively handle difficult samples near category boundaries. Method C enhances transfer performance by aligning cross-domain higher-order feature moments, but its ability to discriminate category boundaries is limited, making fine-grained category differentiation insufficient. Method D sharpens decision boundaries by minimizing margin disparity discrepancy; nevertheless, in practical multi-condition scenarios, its adaptability to cross-domain difficult samples remains inadequate. In contrast, the proposed method establishes a comprehensive fault diagnosis framework for train axle box bearings, integrating data generated by digital twins with multi-source domain adversarial transfer learning. A contrastive learning mechanism is incorporated to improve class separability by pulling similar samples closer while pushing dissimilar samples apart. Importantly, the selection of sample pairs prioritizes difficult samples at category boundaries, allowing the network to learn more refined and discriminative feature representations, thereby significantly enhancing diagnostic accuracy and generalization. In conclusion, comparison with existing methods demonstrates the superiority of the proposed method in diagnosing faults under unseen working conditions.

5. Conclusions

This article proposes a digital-twin-enhanced adversarial transfer learning framework for fault diagnosis of train axle box bearings, which effectively learns from both multi-component digital twin models and limited measurement data. In the proposed framework, a unified feature extraction subnetwork is designed to capture shared representations, while a class classifier and a domain discriminator are adversarially trained to extract domain-invariant features. To fully exploit available supervised information, contrastive learning is incorporated to compact intra-class features and separate inter-class features explicitly. Within this process, a hard example sampling strategy is employed to focus on learning the key features that distinguish different classes, further enhancing feature discriminability. By jointly minimizing classification error, reducing source–target distribution discrepancies, and suppressing domain-specific variations, the framework strengthens the robustness of learned representations and improves cross-domain generalization. Systematic experiments on the subway transmission system demonstrate the feasibility and advantages of the proposed approach.

Acknowledgements

This work was supported by the National Key R&D Program of China (2022YFB4300604).

References

[1]L. Zhao, Y. Chen, Dynamics and fault diagnosis of railway vehicle gearboxes: a review. Journal of Dynamics, Monitoring and Diagnostics, (2024) 83-98.

[2]Z. Chen, H. Wang, Y. Zhou, Y. Yang, Y. Liu, A multiscale feature extraction and fusion method for diagnosing bearing faults. Journal of Dynamics, Monitoring and Diagnostics, 3(4) (2024) 268-278.

[3]S. Chen, L. Guo, J. Fan, C. Yi, K. Wang, W. Zhai, Bandwidth-aware adaptive chirp mode decomposition for railway bearing fault diagnosis. Structural Health Monitoring, 23(2) (2024) 876-902.

[4]A. Glowacz, M. Sulowicz, J. Zielonka, Z. Li, W. Glowacz, A. Kumar, Acoustic fault diagnosis of three-phase induction motors using smartphone and deep learning, Expert Systems with Applications, 262 (2025) 125633.

[5] L. Zhang, J. Qiu, J. Liu, Q. Xiao, C. Wang, P. Zhou, Y. Zhang, C. Sun, Y. Luo, CTNet: an interpretable convolutional neural network for bearing fault diagnosis. Structural Health Monitoring, (2025) 14759217251382151.

[6]A. Ding, Y. Qin, B. Wang, X. Cheng, L. Jia, An elastic expandable fault diagnosis method of three-phase motors using continual learning for class-added sample accumulations, IEEE Transactions on Industrial Electronics, 71 (2023) 7896-7905.

[7]A. Ding, X. Yi, Y. Qin, B. Wang, Self-driven continual learning for class-added motor fault diagnosis based on unseen fault detector and propensity distillation, Engineering Applications of Artificial Intelligence, 127 (2024) 107382.

[8]X. Ren, Y. Qin, B. Li, B. Wang, X. Yi, L. Jia, A core space gradient projection-based continual learning framework for remaining useful life prediction of machinery under variable working conditions, Reliability Engineering & System Safety, 252 (2024) 110428.

[9]H. Wang, J. Xu, R. Yan, Intelligent fault diagnosis for planetary gearbox using transferable deep Q network under variable conditions with small training data, Journal of Dynamics, Monitoring and Diagnostics, 2 (2023) 30-41.

[10]Y. Zhang, J. Ding, Y. Li, Z. Ren, K. Feng, Multi-modal data cross-domain fusion network for gearbox fault diagnosis under variable working conditions, Engineering Applications of Artificial Intelligence, 133 (2024) 108236.

[11]C. Li, L. Mo, C.K. Kwoh, X. Li, Z. Chen, M. Wu, R. Yan, Noise-robust multi-view graph neural network for fault diagnosis of rotating machinery, Mechanical Systems and Signal Processing, 224 (2025) 112025.

[12]F. Huang, K. Zhang, Z. Li, Q. Zheng, G. Ding, M. Zhao, Y. Zhang, A rolling bearing fault diagnosis method based on interactive generative feature space oversampling-based autoencoder under imbalanced data. Structural Health Monitoring, 24(2) (2025) 979-997.

[13]S. Xie, P. Xie, J. Wang, L. Yang, A fault diagnosis method for critical rotating components in trains based on multi-pooling attention convolution and an improved vision transformer. Structural Health Monitoring, 14759217251355472 (2025).

[14]P. Zhang, R. Chen, L. Yang, Y. Zou, L. Gao, Recent progress in digital twin-driven fault diagnosis of rotating machinery: A comprehensive review, Neurocomputing, 634 (2025) 129914.

[15]Y. Qin, H. Liu, Y. Mao, Faulty rolling bearing digital twin model and its application in fault diagnosis with imbalanced samples, Advanced Engineering Informatics, 61 (2024) 102513.

[16]K. Feng, Y. Xu, Y. Wang, S. Li, Q. Jiang, B. Sun, J. Zheng, Q. Ni, Digital twin enabled domain adversarial graph networks for bearing fault diagnosis, IEEE Transactions on Industrial Cyber-Physical Systems, 1 (2023) 113-122.

[17]Y. Pan, C. Yi, X. Liao, Y. Lin, B. Wu, F. Zhang, J. Lin, Fault diagnosis method for high-speed train axlebox bearings based on the joint driving of bearing dynamics simulation and experimental data. Structural Health Monitoring, (2025) 14759217251341855.

[18]Z. Ming, B. Tang, L. Deng, Q. Yang, Q. Li, Q. Ni, Digital twin-assisted fault diagnosis framework for rolling bearings under imbalanced data, Applied Soft Computing, 168 (2023) 112528.

[19]Z. Zheng, D. Song, W. Zhang, X. Xu, C. Ma, W. Cui, Dynamic response analysis of high-speed train axle box bearing by considering time-varying dynamic parameters, Mechanical Systems and Signal Processing, 224 (2025) 112119.

[20]Y. Zhao, T. Sheng, D. Li, Data augmentation fault diagnosis of rolling machinery using condition denoising

diffusion probabilistic model and improved CNN, IEEE Transactions on Instrumentation and Measurement, 74 (2025) 1-12.

[21]M. Long, Z. Cao, J. Wang, M.I. Jordan, Conditional adversarial domain adaptation, Advances in Neural Information Processing Systems, 31 (2018).

[22]X. Peng, Q. Bai, X. Xia, Z. Huang, K. Saenko, B. Wang, Moment matching for multi-source domain adaptation, Proceedings of the IEEE/CVF International Conference on Computer Vision, 32 (2019) 1406-1415.

[23]Y. Zhang, T. Liu, M. Long, M. Jordan, Bridging theory and algorithm for domain adaptation, Proceedings of the International Conference on Machine Learning, 36 (2019) 7404-7413.